TKK Dissertations 176
Espoo 2009

DILUTE HELIUM MIXTURES AT LOW TEMPERATURES: PROPERTIES AND COOLING METHODS

Doctoral Dissertation

Elias Pentti

Helsinki University of Technology
Low Temperature Laboratory

TKK Dissertations 176
Espoo 2009

DILUTE HELIUM MIXTURES AT LOW TEMPERATURES: PROPERTIES AND COOLING METHODS

Doctoral Dissertation

Elias Pentti

Dissertation for the degree of Doctor of Science in Technology to be presented with due permission of the Faculty of Information and Natural Sciences for public examination and debate in Auditorium AS1 at Helsinki University of Technology (Espoo, Finland) on the 31st of August, 2009, at 12 noon.

Helsinki University of Technology
Low Temperature Laboratory

Teknillinen korkeakoulu
Kylmälaboratorio

Distribution:
Helsinki University of Technology
Low Temperature Laboratory
P.O. Box 5100
FI - 02015 TKK
FINLAND
URL: http://ltl.tkk.fi/
Tel. +358-9-451 5619
Fax +358-9-451 2969
E-mail: Elias.Pentti@tkk.fi

ISBN 978-952-248-020-0
ISBN 978-952-248-021-7 (PDF)
ISSN 1795-2239
ISSN 1795-4584 (PDF)
URL: http://lib.tkk.fi/Diss/2009/isbn9789522480217/

TKK-DISS-2630

Multiprint Oy
Espoo 2009

ABSTRACT OF DOCTORAL DISSERTATION	HELSINKI UNIVERSITY OF TECHNOLOGY P. O. BOX 1000, FI-02015 TKK http://www.tkk.fi

Author Elias Mikael Martinpoika Pentti

Name of the dissertation

Dilute Helium Mixtures at Low Temperatures: Properties and Cooling Methods

Manuscript submitted April 17, 2009	Manuscript revised July 28, 2009
Date of the defence August 31, 2009	
☐ Monograph	☑ Article dissertation (summary + original articles)
Faculty	Faculty of Information and Natural Sciences
Department	Low Temperature Laboratory
Field of research	Experimental condensed matter physics
Opponent(s)	Professor Brian Cowan
Supervisor	Professor Matti Kaivola
Instructor	Docent Juha Tuoriniemi

Abstract

This thesis describes experimental work on dilute mixtures of ^{3}He in ^{4}He, mainly at millikelvin temperatures. The isotopic helium mixture has the unique property of remaining a miscible liquid down to the absolute zero temperature. In the mK regime, it consists of two very different components: perfectly superfluid ^{4}He, and a weakly interacting degenerate Fermi liquid of ^{3}He, predicted by theory to undergo transition to the superfluid state at an extremely low temperature. To discover that transition, new ways of cooling helium mixtures need to be developed, as it is not likely that the conventional method of nuclear demagnetization of copper can be improved to reach helium temperatures notably below the temperatures of order 0.1 mK attained so far.

Adiabatic melting of ^{4}He in the presence of liquid ^{3}He is probably the most promising method of cooling helium mixtures to microkelvin temperatures. It produces helium mixture colder than the initial temperature as a direct consequence of the mixing of the isotopes. The starting configuration is attainable by pressurizing liquid helium mixture to its solidification pressure at a temperature below some tens of mK, as only ^{4}He then enters the solid phase. This thesis describes an experiment in which the method of adiabatic melting was, for the first time, realized at sub-millikelvin temperatures, where the superfluidity of the pure ^{3}He phase enables, in principle, a drastic decrease of temperature. In the experiments, cooling from initial temperatures between 0.3 and 0.9 mK was detected, temperature reduction remaining below a factor of two for recognized reasons of a technical rather than fundamental nature.

A capacitive differential pressure transducer, constructed for the experiment, was used for high accuracy measurements of the temperature dependence of the melting pressure of helium mixtures with several ^{3}He concentrations. The melting pressure is suitable for thermometry and carries information on the interactions of ^{3}He particles in the mixture. Also, the response of a quartz tuning fork immersed in helium was studied. Its sensitivity to the properties of the surrounding fluid was utilized to determine the saturation concentration of dilute ^{3}He across the entire accessible pressure range. The tuning fork was found to exhibit a complex pattern of anomalies attributed to resonant modes of second sound, or concentration waves, inside its cylindrical container.

Keywords	helium mixture, superfluid, tuning fork, melting pressure, adiabatic melting, second sound		
ISBN (printed)	978-952-248-020-0	ISSN (printed)	1795-2239
ISBN (pdf)	978-952-248-021-7	ISSN (pdf)	1795-4584
Language	English	Number of pages	42 + app. 112
Publisher	Low Temperature Laboratory, Helsinki University of Technology		
Print distribution	Low Temperature Laboratory, Helsinki University of Technology		
☑ The dissertation can be read at http://lib.tkk.fi/Diss/2009/isbn9789522480217/			

VÄITÖSKIRJAN TIIVISTELMÄ	TEKNILLINEN KORKEAKOULU PL 1000, 02015 TKK http://www.tkk.fi

Tekijä Elias Mikael Martinpoika Pentti

Väitöskirjan nimi

Dilute Helium Mixtures at Low Temperatures: Properties and Cooling Methods
Laimeat heliumseokset matalissa lämpötiloissa: ominaisuuksia ja jäähdytysmenetelmiä

Käsikirjoituksen päivämäärä 17.4.2009	Korjatun käsikirjoituksen päivämäärä 28.7.2009
Väitöstilaisuuden ajankohta 31.8.2009	
☐ Monografia	☑ Yhdistelmäväitöskirja (yhteenveto + erillisartikkelit)

Tiedekunta	Informaatio- ja luonnontieteiden tiedekunta
Laitos	Kylmälaboratorio
Tutkimusala	Kokeellinen materiaalifysiikka
Vastaväittäjä(t)	Prof. Brian Cowan
Työn valvoja	Prof. Matti Kaivola
Työn ohjaaja	Dos. Juha Tuoriniemi

Tiivistelmä

Väitöskirja kuvaa kokeita, joissa tutkittiin ^{3}He:n laimeita seoksia ^{4}He:ssä pääasiassa millikelvinalueella. Heliumisotooppien seoksella on se ainutlaatuinen ominaisuus, että se pysyy nestemäisenä absoluuttiseen nollapisteeseen asti, ja koostuu millikelvinalueella kahdesta hyvin erilaisesta komponentista: täysin suprajuoksevasta ^{4}He:stä ja heikosti vuorovaikuttavasta degeneroituneesta ^{3}He-ferminesteestä, jonka teoria ennustaa muuttuvan supranesteeksi erittäin matalassa lämpötilassa. Tämän transition löytymiseksi on kehitettävä uusia tapoja jäähdyttää heliumseoksia, sillä niitä ei todennäköisesti voida jäähdyttää merkittävästi alle saavutetun 0,1 mK suuruusluokkaa olevan lämpötilan vain parantamalla tavanomaista menetelmää, kuparin ydindemagnetointia.

^{4}He:n adiabaattinen sulaminen ja sekoittuminen ^{3}He-nesteeseen on luultavasti lupaavin menetelmä heliumseosten jäähdyttämiseksi mikrokelvinalueelle. Siinä muodostuva seos on alkulämpötilaa kylmempää, mikä seuraa suoraan isotooppien sekoittumisesta. Alkutila saavutetaan paineistamalla heliumseosta kiinteytymispaineeseensa muutaman kymmenen mK alapuolella, jolloin ainoastaan ^{4}He siirtyy kiintään faasiin. Väitöskirja kuvaa koetta, jossa adiabaattisen sulamisen menetelmää sovellettiin ensi kertaa alle 1 mK lämpötiloissa, joissa ^{3}He:n suprajuoksevuus periaatteessa mahdollistaa lämpötilan dramaattisen putoamisen. Kokeissa jäähtymistä havaittiin alkulämpötiloista, jotka vaihtelivat välillä 0,3–0,9 mK. Lämpötilan suhteellinen lasku jäi alle tekijään kaksi, mihin oli tunnistettavat ja enemmän tekniset kuin periaatteelliset syyt.

Koetta varten valmistettua kapasitiivista paine-eroanturia käytettiin hyvin tarkkoihin heliumseosten sulamispaineen lämpötilariippuvuuden mittauksiin useilla pitoisuuksilla. Sulamispaine soveltuu lämpötilan mittaamiseen ja välittää tietoa seoksessa olevien ^{3}He-hiukkasten välisistä vuorovaikutuksista. Kokeessa tutkittiin myös näytteeseen upotetun kvartsihaarukan värähtelyvasteen riippuvuutta ympäröivän heliumin ominaisuuksista, ja määritettiin sen avulla laimean ^{3}He:n kyllästyspitoisuus koko saavutettavissa olevalla painealueella. Haarukan vasteessa havaittiin monimutkainen sarja poikkeamia, joiden ymmärretään johtuvan toisen äänen eli konsentraatioaaltojen resonoivista moodeista haarukan lieriömäisessä kotelossa.

Asiasanat	heliumseos, supraneste, kvartsihaarukka, sulamispaine, adiabaattinen sulaminen, toinen ääni
ISBN (painettu) 978-952-248-020-0	ISSN (painettu) 1795-2239
ISBN (pdf) 978-952-248-021-7	ISSN (pdf) 1795-4584
Kieli englanti	Sivumäärä 42 + liit. 112
Julkaisija	Kylmälaboratorio, Teknillinen Korkeakoulu
Painetun väitöskirjan jakelu	Kylmälaboratorio, Teknillinen Korkeakoulu
☑ Luettavissa verkossa osoitteessa http://lib.tkk.fi/Diss/2009/isbn9789522480217/	

Contents

Preface

I feel privileged for having had the opportunity to work for ten years at the Low Temperature Laboratory, studying the fascinating physics of ultracold helium with world-class scientists and state-of-the-art equipment. I wish to express my gratitude to Professor Mikko Paalanen, the director of the laboratory, and to Docent Juha Tuoriniemi, the instructor of my theses and the leader of YKI group, for guiding me along the way through my studies. I am also indebted to Dr. Alexander Sebedash, whose expertise was crucial for the experiments that are the basis of this Thesis.

I have been a member of a community where research, in addition to aiming at success through hard work, can also be fun. I want to thank all my fellow students of low temperature physics for companionship and cooperation, especially Anssi Salmela and Juha Martikainen who have contributed greatly to the results presented in this Thesis. Both the encouraging example of preceding graduate students and the refreshing company of younger generations have been invaluable to me, as well as the help of the technical and administrative personnel of the laboratory in various stages of my work.

Completing my graduate studies concludes not just a decade at the Low Temperature Laboratory but also a quarter of a century of education altogether. Throughout that time, the loving support of my parents has been indispensable, although its form has naturally changed a lot since my first day at school back in August 1984. I am also fortunate to have a great little brother and three splendid sisters, two of which have even chosen to follow me to study at TKK. Their value as friends has only been revealed after moving away from the childhood home.

Finally, I thank my dear wife Laura from my heart for her enduring love for me and confidence in the eventual completion of this work, and our wonderful daughter Selma for the joy she has brought into our life. During the sometimes difficult process of preparing this Thesis, they have reminded me of that, after all, the phenomena that really matter occur at about 310 K.

List of publications

This Thesis is based on the following original publications, which will be henceforth referred to by the respective Roman numeral.

I Juha Tuoriniemi, Juha Martikainen, Elias Pentti, Alexander Sebedash, Sergey Boldarev, and George Pickett. *Towards Superfluidity of ^{3}He Diluted by ^{4}He*. Journal of Low Temperature Physics **129**, 531–545 (2002). DOI: 10.1023/A:1021468614550

II E. Pentti, J. Tuoriniemi, A. Salmela, and A. Sebedash. *Melting Pressure Thermometry of the Saturated Helium Mixture at Millikelvin Temperatures*. Journal of Low Temperature Physics **146**, 71–83 (2007). DOI: 10.1007/s10909-006-9267-8

III A. P. Sebedash, J. T. Tuoriniemi, S. T. Boldarev, E. M. M. Pentti, and A. J. Salmela. *Adiabatic Melting of ^{4}He Crystal in Superfluid ^{3}He at Sub-millikelvin Temperatures*. Journal of Low Temperature Physics **148**, 725–729 (2007). DOI: 10.1007/s10909-007-9443-5

IV A. P. Sebedash, J. T. Tuoriniemi, E. M. M. Pentti, and A. J. Salmela. *Osmotic Pressure of ^{3}He–^{4}He Solutions at 25.3 Bar and Low Temperatures*. Journal of Low Temperature Physics **150**, 181–186 (2008). DOI: 10.1007/s10909-007-9535-2

V E. M. Pentti, J. T. Tuoriniemi, A. J. Salmela, and A. P. Sebedash. *Quartz Tuning Fork in Helium*. Journal of Low Temperature Physics **150**, 555–560 (2008). DOI: 10.1007/s10909-007-9583-7

VI Elias M. Pentti, Juha T. Tuoriniemi, Anssi J. Salmela, and Alexander P. Sebedash. *Solubility of ^{3}He in ^{4}He at millikelvin temperatures up to the melting pressure measured by a quartz tuning fork*. Physical Review B **78**, 064509 (2008). DOI: 10.1103/PhysRevB.78.064509

VII Elias Pentti, Juho Rysti, Anssi Salmela, Alexander Sebedash, and Juha Tuoriniemi. *Studies on helium liquids by vibrating wires and quartz tuning forks*. Report TKK-KYL-021 (2009). 36 pages.

Author's contribution

The publications in this Thesis are results of team work by the YKI group at the Low Temperature Laboratory.

The author was liable for the numerical thermal modeling related to the experiment on cooling dilute helium mixtures by nuclear demagnetization, discussed in publication **I**, as well as for the compilation of the computer program necessary for the vibrating wire measurements in that experiment. The development and maintenance of the measurement program continued throughout the rest of the work and remained a specific responsibility of the author.

As a part of the preparations for the experiment on cooling by adiabatic melting of ^{4}He, the author designed and constructed the high-pressure gas handling system outside the cryostat. During the experiment, he participated in operating the cryostat, performing the measurements, and analyzing the data presented in publication **III**. Publication **II** was written by him.

During the third experiment covered by this Thesis, the author shared the day-to-day duties at the cryostat with the other members of the group and had an active role in planning and performing the measurements, particularly those made by the quartz tuning fork, but also the pressure measurements on the partly solidified helium mixture [**IV**]. The author wrote publications **V** and **VI**, based on his analysis of the obtained tuning fork data. Publication **VII**, which presents results from all the three experiments mentioned above, was also written by him.

Chapter 1

Introduction

Helium is the second lightest and the second most abundant element in the universe next to hydrogen. It has two stable isotopes: the heavier ^{4}He, by far more common on earth, and the lighter ^{3}He. As a noble gas, helium does not form chemical compounds but always exists as monatomic substance, and due to its small atomic mass and weak interatomic interaction, liquefies at temperatures so low (^{4}He at 4.2 K at the atmospheric pressure) that all other matter can only exist as solid or extremely sparse gas. Moreover, helium has a unique property that has made it a major subject of low-temperature research for over a century: it remains liquid down to the absolute zero temperature unless compressed to a substantial pressure (2.53 MPa for pure ^{4}He and 3.44 MPa for pure ^{3}He), and even more interestingly, undergoes a transition from a normal liquid to a superfluid.

Although chemically identical, the two helium isotopes behave very differently at low temperatures due to the fundamental quantum mechanical difference between the fermionic ^{3}He and bosonic ^{4}He. The difference of three orders of magnitude between their superfluid transition temperatures is a concrete indication of this. In the liquid phase, the isotopes do not mix at arbitrary proportions below a certain temperature (0.87 K at saturated vapor pressure) but the mixture separates into two phases, one dilute and the other rich in ^{3}He. As atoms of both isotopes are more strongly bound to liquid ^{4}He than to ^{3}He, the equilibrium composition of the ^{3}He-rich mixture converges into pure ^{3}He in the zero-temperature limit, whereas in the dilute mixture, the concentration of ^{3}He saturates to a pressure-dependent non-zero value. In the millikelvin regime, ^{4}He in the mixture is essentially in its ground state, a perfect superfluid, whereas the diluted ^{3}He forms a unique weakly interacting uncharged Fermi liquid, whose particle density can be adjusted continuously over a wide range, and which can

be studied at temperatures from above its Fermi temperature down to the degeneracy region.

It is anticipated that like pure ^{3}He, the diluted ^{3}He also experiences Cooper pairing and thus superfluidity at a yet undiscovered, extremely low temperature. In pursuit of this goal, helium mixtures have been reportedly cooled to 97 μK by Oh *et al.*[1], and in the experiment at the Low Temperature Laboratory in Otaniemi, discussed in publication **I**, numerical thermal modeling indicated temperatures somewhat lower than that but definitely above 10 μK [2]. That experiment, as well as the two subsequent runs described in this Thesis, were conducted in the YKI cryostat, which combines efficient ^{3}He–^{4}He dilution refrigeration with adiabatic nuclear demagnetization cooling of copper [3]. This cryostat holds the low temperature record of 0.1 nK for nuclear spins of rhodium, reached by employing two nuclear demagnetization stages in series [4]. Although temperatures of that order can only be produced among the nuclei of the demagnetization stage, coupling other samples thermally to a massive copper nuclear stage is the conventional method of reaching sub-millikelvin temperatures in condensed matter. This technique was applied in both mixture experiments mentioned above and has been used in many milestone experiments, such as discovering the superconductivity in non-compressed lithium below 0.4 mK by us [5], and at Lancaster University in studies of superfluid ^{3}He down to below 0.1 mK [6].

When cooling helium by means of nuclear demagnetization, the main factor governing the minimum attainable sample temperature is the thermal boundary resistance, or Kapitza resistance, at the interface between the liquid and any metallic parts coupled to or forming the nuclear stage. Sintered metal powder with a large surface area is commonly used to improve the thermal coupling, but because the Kapitza resistance increases steeply as temperature falls, there remains a practical minimum temperature where the inevitable heat leak to the sample is only just absorbed by the nuclear stage, regardless of how low the temperature of the copper nuclei is. Therefore, it is evident that improvements of this cooling method are unlikely to significantly reduce the attainable temperature of helium samples, and that reaching even the highest theoretical predictions of the superfluid transition temperature of diluted ^{3}He, lying in the low microkelvin range, requires a completely different method of cooling. This Thesis describes an experiment on probably the most promising such method, the adiabatic melting of ^{4}He in the presence of liquid ^{3}He, a process in which cooling of the forming mixture is based on the heat of mixing directly [7]. The method was, for the first time, realized below 1 mK, with encouraging results.

Determining the temperature of the sample is an essential part of any cooling experiment. At sub-millikelvin temperatures, thermometry of helium must rely

on measuring its properties directly because external thermometers rapidly lose thermal contact with the sample as temperature falls. In the experiments described in this Thesis, two direct methods of monitoring the state of helium were applied: first, melting pressure measurement, and second, immersed mechanical resonators in the form of vibrating metal wires and quartz tuning forks.

Melting pressure measurements on dilute helium mixtures were done by a differential pressure gauge using the melting pressure of pure ^{4}He as a reference. The melting pressure of the phase-separated mixture present in the adiabatic melting experiment depends uniquely on temperature and provides an alternative to the pure ^{3}He melting pressure thermometry, the basis of the current provisional definition of the temperature scale in the millikelvin range [8]. In the last part of this work, melting pressures of mixture samples with different concentrations were measured to obtain data useful for developing theoretical models of interactions between ^{3}He atoms in the mixture.

Vibrating wire resonators are a standard instrument in low-temperature helium research, and were employed in our nuclear demagnetization cooling experiment [9, 10, 11] as well as in the experiment on adiabatic melting. Quartz tuning forks, on the other hand, are a relatively new tool in this field [12, 13] and were incorporated into our work in the last experiment of this Thesis. We studied the response of a quartz fork in various phases of helium as a function of temperature, pressure, and ^{3}He concentration of dilute helium mixture.

Chapter 2

Experiments

2.1 Cooling by adiabatic melting of ^{4}He in ^{3}He

2.1.1 Principle of the method

Cooling helium mixture by adiabatic melting of ^{4}He is based on the same principle as the ^{3}He–^{4}He dilution refrigerator: when ^{3}He transfers from its rich phase (essentially pure ^{3}He at millikelvin temperatures) to a dilute mixture, an amount of energy, the heat of mixing, is absorbed because the enthalpy of ^{3}He is larger in the former phase than in the latter. One crucial difference of the methods is that in a dilution refrigerator, the process can be made continuous and is based on circulation of ^{3}He, whereas adiabatic melting is a one-time event, in which solid ^{4}He melts in the presence of liquid ^{3}He. The process can be repeated in cycles, of course.

Figure 2.1 illustrates the thermodynamics of adiabatic melting by temperature plots of the entropy of a mixture of ^{3}He and ^{4}He in the two extreme configurations present in the process: a homogeneous liquid mixture, and with the isotopes completely separated into solid ^{4}He and liquid pure ^{3}He. The latter is the equilibrium state of a helium mixture in the millikelvin regime above its melting pressure [14]. The entropy of ^{4}He, arising mainly from phonons, is vanishingly small in both configurations compared with ^{3}He, and can be neglected. As degenerate Fermi systems, both ^{3}He in the mixture and the pure ^{3}He above its superfluid transition temperature T_c (about 2.4 mK at the relevant pressure) possess entropies proportional to T, whereas in superfluid ^{3}He, entropy has a

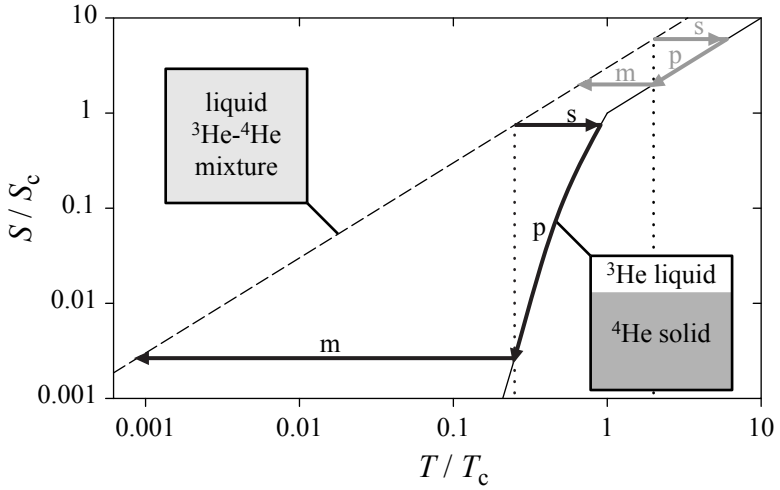

Fig. 2.1 Principle of cooling by adiabatic melting of ^{4}He in ^{3}He. Entropy of equal amounts of ^{3}He in a mixture (dashed line) and pure phase (unbroken line), and arrows representing the three stages of an ideal cooling process, starting from $T_c/4$ (black) and 2 T_c (gray): separation of isotopes by solidification of ^{4}He (s), precooling (p), and mixing due to melting of ^{4}He (m).

much steeper temperature dependence, calculated for this plot from heat capacity measurements of Greywall [15]. The mixture phase is assumed not to become superfluid in the presented temperature range, and to have a Fermi temperature one-third of that of the pure phase, corresponding roughly to a saturated mixture at the melting pressure. The temperature is scaled by T_c, and entropy by S_c, the values for the pure ^{3}He phase at the superfluid transition.

Figure 2.1 also presents the stages of cooling by adiabatic melting, starting from two example temperatures, 2 T_c (gray arrows) and $T_c/4$ (black arrows). The first stage (marked 's') is the separation of the helium isotopes by solidifying ^{4}He, which is achieved by pressurizing the sample. At this stage, temperature rises because forming the pure ^{3}He phase releases heat. That heat is removed during the precooling stage (marked 'p') by an external thermal bath or cooling device, bringing the system back to the initial temperature. Finally, in the melting stage ('m'), pressure is lowered, the solid ^{4}He melts and mixes with the ^{3}He. In the ideal case of the melting and mixing proceeding adiabatically, *i.e.*, without dissipation or exchange of energy with the environment, the final temperature of the resulting mixture is lowered according to the entropy diagram. Starting from above T_c, the maximum cooling factor is the ratio of the Fermi temperatures, but below T_c, the ratio increases rapidly, being almost 300 in the example presented

by black arrows. In practice, however, this ideal is not reached for several reasons. To mention a few, heat leak and dissipation due to viscous flow of ^{3}He can never be totally avoided, there may be parasitic heat capacity involved such as some remnant mixture as a result of incomplete solidification of ^{4}He, and the thermal coupling to the environment, necessary for precooling, starts to warm up the sample as soon as it has become the coldest part of the system.

The adiabatic melting method has been experimented by Sebedash in Moscow at temperatures between 30 and 150 mK, achieving cooling ratios of order two [16]. Our experiment was the first realization of the method below 1 mK with superfluid ^{3}He.

2.1.2 Apparatus

Figure 2.2 shows the experimental cell for adiabatic melting. The mixture volume of 78 cm^3 has a flat dish-like shape to reduce the viscous heating by ^{3}He flowing from the pure ^{3}He phase, floating on top, to mix with the ^{4}He released from the solid, which forms on the bottom of the cell because it is denser than the liquid phases. The walls of the cell consist of two concave copper parts, pressed together by robust bronze clamps. The rather massive structure of the cell aims at preventing changes of its shape under the high working pressure. The cell was mounted in the cryostat and thermally connected to the nuclear demagnetization stage for cooling to sub-millikelvin temperatures.

To control the solidification and melting of the sample, its pressure had to be varied around the melting pressure. An ordinary filling line could not have been used for that purpose because of the minimum of the melting pressure of dilute helium mixtures, occurring around 1 K for all concentrations [17]. Bellows or other variable-volume arrangements, common in experiments on solid ^{3}He also having a melting pressure minimum, were also excluded to avoid possible sources of dissipation. Instead, pressure control was provided by a superleak line, parallel to the ordinary filling capillary. The superleak is a tube tightly packed with fine powder, permeable to superfluid ^{4}He but not to normal ^{3}He, thus allowing selective removal and addition of ^{4}He to lower or raise the pressure. Moreover, as the melting pressure of ^{4}He is increased by the constricted porous geometry of the superleak, it remains open at the experimental pressures above the low-temperature melting pressure of pure bulk ^{4}He. The warmer end of the superleak, from which the line continues towards room temperature as an ordinary tube, was coupled to the still plate of the dilution refrigerator ($T \approx 0.75$ K) via a modest thermal resistance and equipped with a heater. Thus, it was

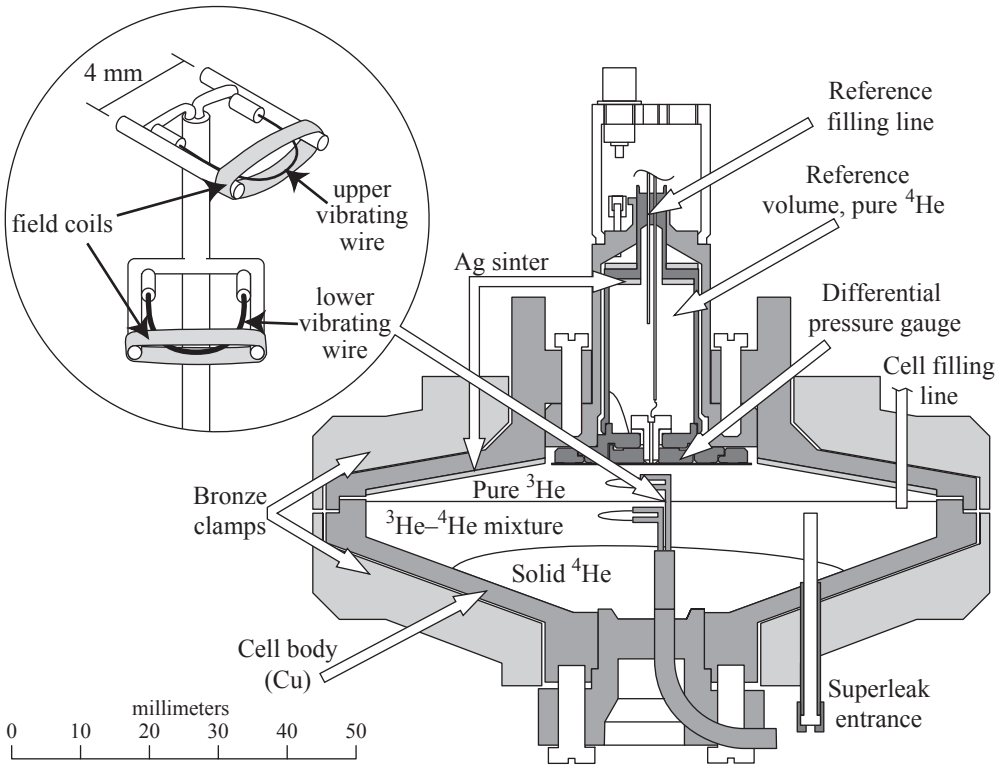

Fig. 2.2 Cross section of the adiabatic melting cell and a blow-up view of the double vibrating wire installation.

possible to adjust the temperature of the end of the superleak, either to the range where bulk ^{4}He is superfluid and the line is open ($T \approx 1.5$ K), or to allow it to become blocked by solid ^{4}He ($T < 1.2$ K) (see Fig. 2.3).

The experimental setup includes three methods of thermometry: vibrating wires immersed in the sample, a pulsed Pt-NMR thermometer attached to the cell body, and melting pressure thermometry. Resistor thermometers and a ^{60}Co nuclear orientation thermometer at the mixing chamber could also be used when the cell and the nuclear stage were in thermal contact with the dilution refrigerator. There are two vibrating wires in the cell, an upper one for ^{3}He and a lower one for mixtures, installed as a unit also including the coils producing the static magnetic fields needed for their operation. This is necessary because the cell is not in an external magnetic field. Both the vibrating wires and the Pt-NMR thermometer are described in detail in Ref. [18], and publication **VII** discusses results obtained by the vibrating wires.

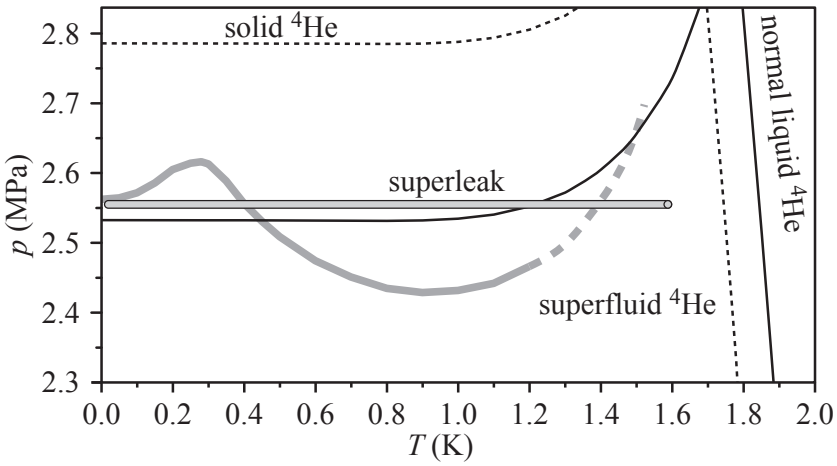

Fig. 2.3 Diagram of the helium phases at the ends and inside the superleak line: melting and superfluid transition curves of ^{4}He in bulk (solid black lines) and in the pores of the superleak (schematic, dashed line); melting curve of mixture with 9.4 % of ^{3}He (above saturation at $T < 0.2$ K) by Lopatik [17] (gray).

For measuring the melting pressure of the mixture, the cell is equipped with a differential pressure transducer. Its sensing element is a BeCu membrane separating the mixture volume from a smaller reference volume. Deflection of the membrane was detected by measuring the capacitance between it and the central part of the planar bottom of the reference volume. The reference volume was filled by pure ^{4}He, which was partially solidified to provide an essentially temperature-independent reference pressure of 2.53 MPa, less than 40 kPa below the melting pressure of the saturated mixture at $T = 0$. Thus, the pressure transducer could be designed for pressures almost two orders of magnitude smaller than the absolute pressure level, which improved its accuracy accordingly to a resolution better than 10 mPa [19]. Results on melting pressures will be discussed in Section 2.3.

2.1.3 Results

Figure 2.4 presents four cases of testing the cooling by adiabatic melting, labeled ‘a’ to ‘d’, as time plots of the temperatures of the helium, measured by the upper vibrating wire in ^{3}He, and of the cell wall, measured by the Pt-NMR thermometer. The plots also show the flow of ^{4}He out of the cell through the superleak,

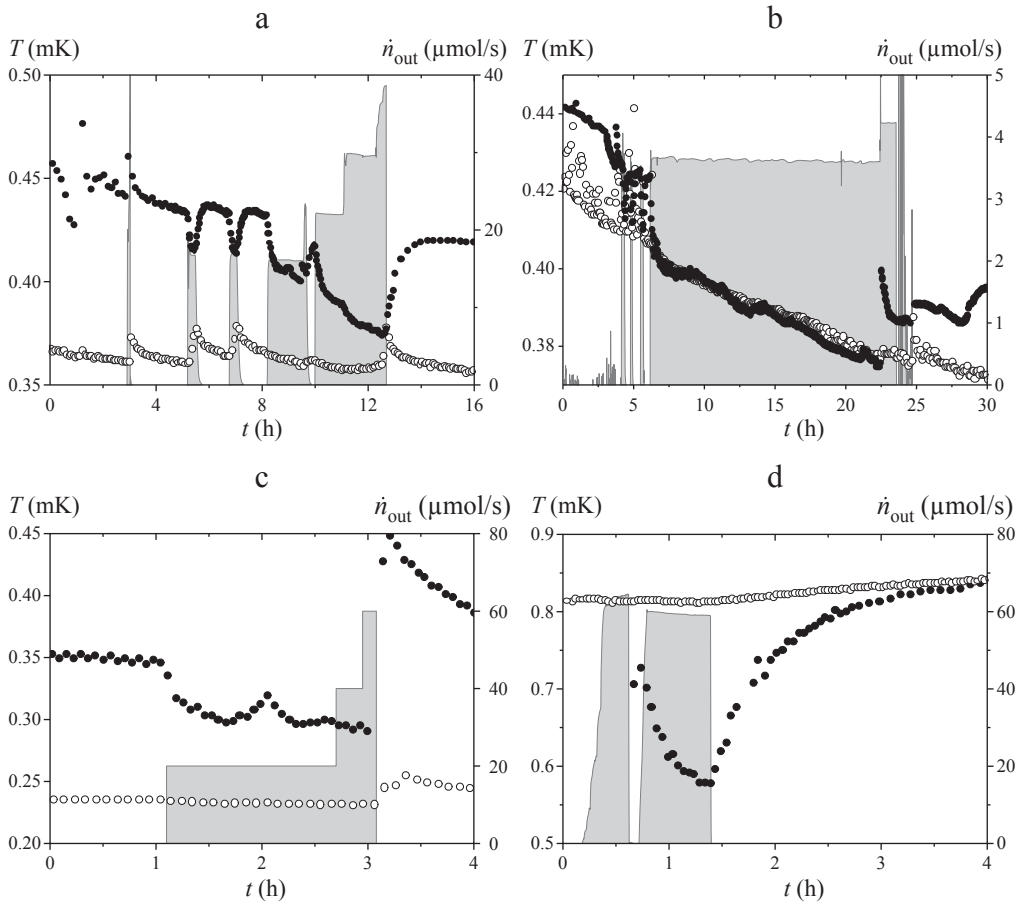

Fig. 2.4 Four adiabatic melting experiments. Temperatures (scale of the left): sample, measured by the vibrating wire in pure ^{3}He (•), cell wall by the Pt-NMR thermometer (○). Melting of the ^{4}He crystal was induced by the flow of ^{4}He (plotted as gray area, scale on the right) out of the superleak line. The zero of each time axis is an arbitrary moment of time shortly before the start of the cooling attempt.

proportional to the melting rate of the ^{4}He crystal and thus to the mixing rate of the isotopes.

In case 'a', the first brief melting at $t = 3$ h was soon halted because of heating of the cell wall. After a few hours, two attempts at a lower melting rate resulted in a noticeable decrease of the liquid temperature, but were accompanied with an increase at the wall. After $t = 8$ h, melting was continued for a longer period as no wall heating occurred. Helium flow rate was increased in steps, leading to the liquid temperature decreasing correspondingly. Eventually, when the helium

flow approached 40 μmol/s, the cell wall started to warm up and the melting was stopped.

In case 'b', there were three short initial periods of melting which all caused wall heating, but when the melting was resumed at the same low rate for the fourth time, no heating occurred, and the process could be continued for almost 20 hours. According to the temperatures measured, the slow melting of ^{4}He kept the liquid at the same temperature with the cell wall, and their initial temperature difference was restored as soon as the melting stopped.

Case 'c' was the one with the lowest temperature of the cell wall. The resonance width of the vibrating wire in ^{3}He was already close to saturating to the vacuum value, so that the liquid temperature calculated from it must be considered merely suggestive. However, the data indicate that the liquid temperature decreased and the wall temperature remained steady until the ^{4}He flow rate was raised from 40 to 60 μmol/s.

Case 'd' is also discussed in publication **III**. Here the temperature is higher and, consequently, thermometry of the liquid by the vibrating wire more reliable than in the other cases. Due to the higher temperature, the cooling power at a given mixing rate was also higher. Together with reaching a ^{4}He flow rate above 50 μmol/s without heating effects, this resulted in the only incident of the liquid temperature certainly falling below the wall temperature. At the beginning of this test, the ^{4}He crystal was rather small and most of the ^{4}He in the cell was already in the liquid mixture phase, giving rise to a significant heat capacity responsible of the long relaxation times visible in the data.

The heating associated with flow of ^{4}He out of the cell through the superleak, most clearly visible in case 'a', was a typical problem in the experiment. The heating occurred somewhere along the superleak line and not inside the cell, which is evident from the fact that an increase of temperature was first detected by either the Pt-NMR thermometer or thermometers at the mixing chamber of the dilution refrigerator, while the temperature of the sample was still falling as a result of cooling by adiabatic melting. The exact reason of the behavior remained unclear, but we learnt to "train" the superleak by brief bursts of ^{4}He out of the cell to allow subsequent lossless outward flow, albeit at a rate somewhat lower than intended. This limitation, together with uncomplete solidification of ^{4}He and a lower than expected thermal boundary resistance between the cell body and the sample, were the causes of the cooling results being rather modest in comparison with the theoretical potential of the method.

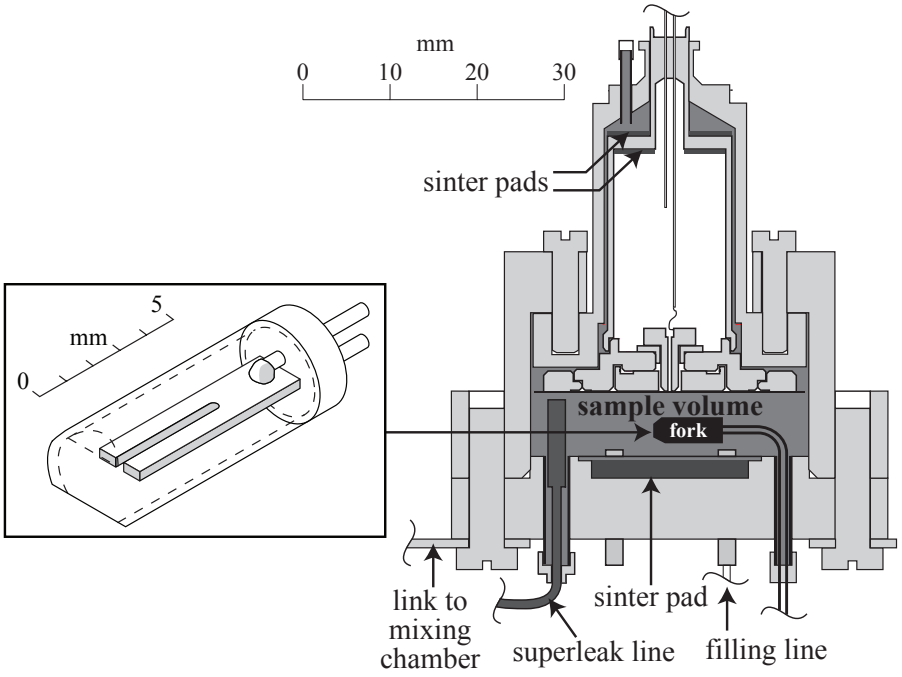

Fig. 2.5 Cross section of the testing cell and a perspective cutaway view of the tuning fork in its container.

2.2 Quartz tuning fork measurements

After the adiabatic melting experiment, three new superleak lines were prepared to find an improved design free of the heating effects. For testing them, a smaller experimental cell, shown in Fig. 2.5, was constructed by attaching a cylindrical chamber with a volume of about 8.3 cm^3 to the differential pressure transducer. A commercial quartz tuning fork (Fox Electronics NC38 [20]) was installed into the cell, leaving the original casing of the fork in place but opening it by grinding two holes at the end. The frequency and width of the fork resonance were determined either from whole resonance spectra or by a single frequency method described in publication **VII**. This setup was used to study the response of the tuning fork in various helium phases across a wide range of temperatures and pressures, as well as for melting pressure measurements of dilute helium mixtures at mK temperatures. The combination of an ordinary filling line and superleak lines in parallel enabled gradual addition of ^{3}He into the cell, first filled by pure ^{4}He, by introducing ^{3}He through the filling line and removing a corresponding amount of ^{4}He through a superleak.

2.2.1 Fluid density

The effect of a fluid surrounding a tuning fork or any other mechanical oscillator is basically observed as a reduction of the resonance frequency from its value in vacuum, indicating an increase in the inertia of the oscillator, and as widening of the resonance peak, which signals damping. In inviscid media, the resonance frequency f_0 can be expected to depend on the fluid density ρ_{fluid} according to

$$f_0 = f_{0,\text{vac}} \left(1 + B \frac{\rho_{\text{fluid}}}{\rho_{\text{fork}}} \right)^{-1/2}, \tag{2.1}$$

with $f_{0,\text{vac}}$ the vacuum resonance frequency, ρ_{fork} the density of the fork, and B a dimensionless geometrical factor of order unity. In the case of an infinite cylinder immersed in an inviscid fluid, B can be determined analytically; it equals one if the fluid is assumed incompressible, and if compressibility is taken into account, becomes a function of the ratio of the radius of the cylinder to the wavelength of sound in the fluid at the oscillating frequency.

In the complicated fork geometry, the exact value of B is difficult to predict, as there are differences from the cylindrical case that are known to have opposite effects on the additional inertia: it is, on one hand, enhanced by the rectangular cross-section and nearby container walls, but on the other hand, reduced because the tines of the fork end in the middle of the surrounding fluid and are elongated in the direction of motion [21].

Our fork measurements allow us to determine B for its geometry by Eq. (2.1) in different phases of helium, as superfluid ^{4}He has no viscosity and data obtained in viscous phases can be extrapolated to the inviscid limit with sufficient accuracy. Publication **V** addresses this issue and shows that, indeed, the relation between the resonance frequency of the fork and the helium density cannot be explained by a single constant value of B but compressibility has to be accounted for. The solvable cylindrical case suggests that the observed values of B can be expected to represent a function of the wavelength of sound, λ; therefore, Fig. 2.6 presents the results as a function of wave number $k = 2\pi/\lambda$, showing data for liquid ^{3}He and ^{4}He at millikelvin temperatures across the pressure range from zero to melting pressure of ^{4}He, liquid ^{4}He at saturated vapor pressure above $T_\lambda = 2.17$ K, and ^{4}He vapor. Values of density and speed of sound in the various helium phases are known from literature [22, 23, 24, 25]. There appears to exist a dependence on k common to all phases studied, saturating to slightly below 1 in the incompressible limit $k \to 0$.

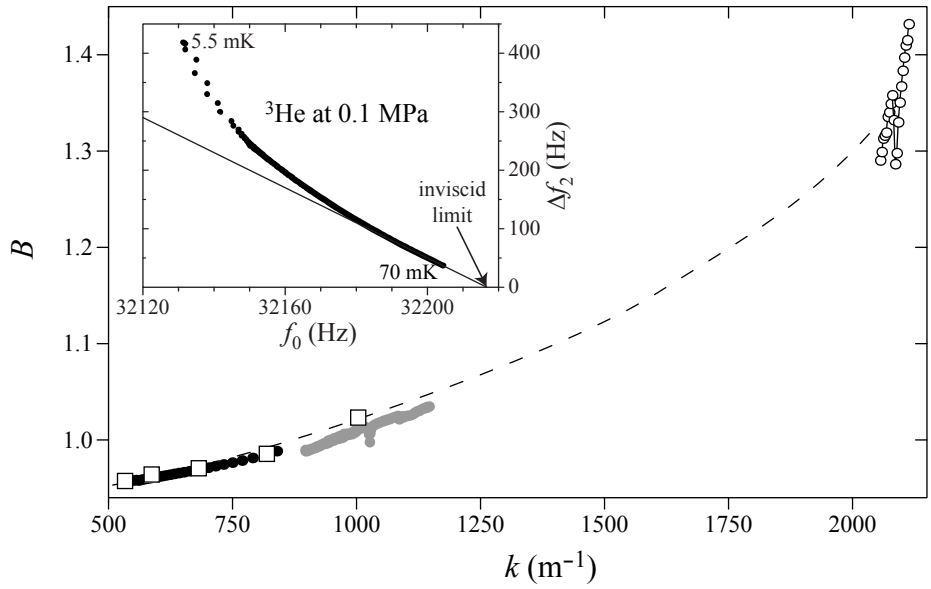

Fig. 2.6 B as a function of wave number k in four helium fluids: liquid ^{3}He (squares) and ^{4}He (black dots) at mK temperatures and different pressures, liquid ^{4}He above T_λ (gray dots), and ^{4}He vapor (circles). Insert: example of obtaining the inviscid limit of resonance frequency from ^{3}He data by extrapolation to vanishing resonance width.

2.2.2 Thermometry

One of the main reasons for incorporating quartz tuning forks into helium research is using them for thermometry in a similar fashion as vibrating wires. Forks have the disadvantage that due to their rectangular geometry, there is no analytical description of the effect of the surrounding fluid to the resonance of the fork, but their ease of use, availability as a standard electronic component, and low intrinsic damping improving the sensitivity to low-viscosity media such as ^{3}He much below T_c, make them an attractive substitute to vibrating wires [12].

Figure 2.7 presents the temperature dependence of the resonance width of the tuning fork in saturated helium mixtures at four pressures. Similarly with vibrating wires, there is a temperature range, about 5 to 50 mK, where the resonance width decreases regularly, almost linearly in a log-log plot, albeit not as steeply as theory for cylindrical wires predicts—a discrepancy also reported by Clubb *et al.* [13] and illustrated in the plot by a theoretical curve calculated by the slip theory for vibrating wires [26, 27, 28]. Above about 50 mK in saturated mixtures and even below that with lower concentrations, the fork exhibited a feature not found by vibrating wires: there appears a multitude of peaks in the resonance

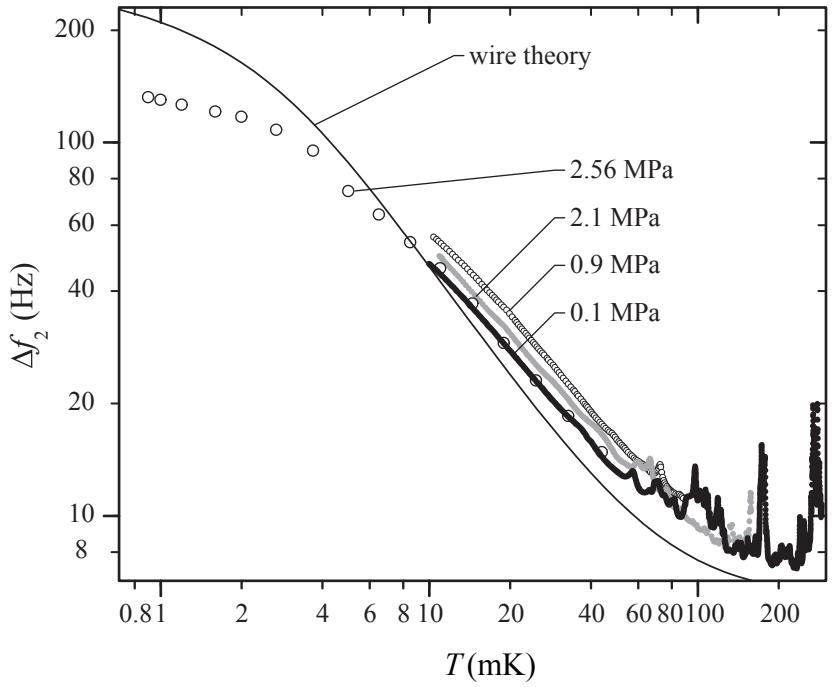

Fig. 2.7 Resonance width Δf_2 of the tuning fork in saturated helium mixture at four pressures shown on the plot, and a curve calculated by theory for vibrating wires.

width data as a function of temperature, which were confirmed to arise from resonances of second sound in the mixture near the fork. Second sound and its effects are discussed further in the next section. At temperatures below 5 mK, to which range we cooled the test cell only once with the sample at melting pressure, the resonance width saturates as a result of the system passing from the hydrodynamic regime to the ballistic regime, where the mean free path of ^{3}He quasiparticles becomes larger than the size of the oscillator.

In pure ^{3}He, we observed a temperature dependence of the resonance width in the hydrodynamic regime that agrees with theory for wires notably better than the mixture data [**VII**]. This leads to conclude that the anomaly in mixtures does not arise from the nontrivial geometry of the forks alone but, perhaps, from temperature-dependent dissipation through emission of second sound which adds to the viscous damping.

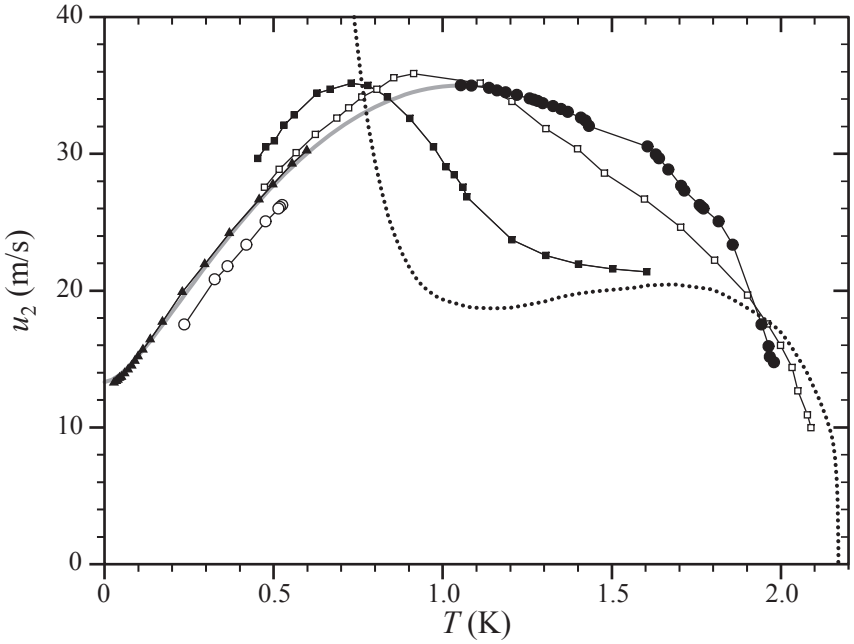

Fig. 2.8 Velocity of second sound u_2 in ^{4}He (dotted line) [29, 30, 31] and mixtures: 0.32 % (■) and 4.3 % (□) at SVP after King and Fairbank [32], 6.278 % (▲) at SVP after Brubaker *et al.* [33], and our estimates for 8 % mixture at SVP above 1.05 K (•) and saturated mixture at melting pressure (○), based on tuning fork data and the assumed dependence below 1.05 K (gray curve).

2.2.3 Second sound

Second sound is the name given to the propagating vibrational mode in a mixture of a superfluid and a normal fluid in which the local densities of the constituents oscillate in opposite phases. Total density varies very little if at all, in contrast to first (ordinary) sound. In pure ^{4}He second sound appears as temperature waves because of the correspondence between temperature and the proportion of the normal and superfluid components, and in dilute helium mixtures as ^{3}He concentration waves. Figure 2.8 shows a plot of some published velocities of second sound in ^{4}He and dilute mixtures as a function of temperature, as well as values deduced from our tuning fork data. Second sound had a remarkable effect on our measurements, rather unexpectedly, because its wavelength at the resonance frequency of the fork is of the order of 1 mm, the typical length scale of the fork and its container. As a result of this coincidence, there is a great number of resonant modes of second sound in the vicinity of the fork that are excited when the frequency of the fork, second sound velocity, and a characteris-

tic dimension of the resonant cavity match. Such modes were detected as sharp peaks in the apparent resonance width of the fork, accompanied with a shift of the resonance frequency also. With a mixture sample of nominally 8% of ^{3}He, we scanned almost the whole temperature range from 0 to 2 K, where ^{4}He in the mixture is superfluid and second sound exists, and obtained the resonance mode pattern presented in Fig. 2.9. Parts of the same spectrum, positions and absolute heights of the peaks varying but order and main features remaining the same, were detected in measurements at different concentrations and pressures.

It is remarkable that at about 1.05 K, there is a reflection point after which the pattern starts to repeat itself in reverse order. This results from the second sound velocity reaching a maximum at that temperature, and can be used to find temperatures of equal velocity below and above the maximum. As published results allow a fairly reliable approximation of second sound velocity in the 8% mixture below the maximum (curve shown in gray), comparison of peaks in the fork data yields the plotted data in Fig. 2.8 for higher temperatures and for the saturated mixture at melting pressure.

2.2.4 Solubility of ^{3}He in ^{4}He

The concentration of ^{3}He in the dilute mixture, conventionally expressed as $x = n_3/(n_3+n_4)$, where n_3 and n_4 are the molar quantities of the helium isotopes, is a key parameter in both experimental and theoretical studies of helium mixtures. Its saturation value x_s depends notably on pressure, with the zero-temperature limit lying at about 0.065 at low pressures and reaching a maximum of about 0.095 near 1 MPa [34].

None of the previously published measurements of x_s extend to the melting pressure of the saturated mixture, probably because of the practical difficulty of reaching that pressure through blocking filling capillaries. Our test setup was suitable for obtaining the lacking data, firstly, because the melting pressure was attainable, and secondly, by exploiting the sensitivity of the tuning fork to the mass density of the mixture. Measurements in mixtures of several concentrations below saturation were performed across the whole pressure range to enable interpretation of the fork response in terms of concentration, so that the saturation concentration could be calculated from data obtained in phase-separated mixture. The measuring temperature was 10 mK, sufficiently low for the observed concentration to be considered as the zero-temperature value. The effect of inevitable minor fluctuations about the nominal temperature was removed from the fork response by using the combination $f_0 + \Delta f_2/4$ as an indicator of the

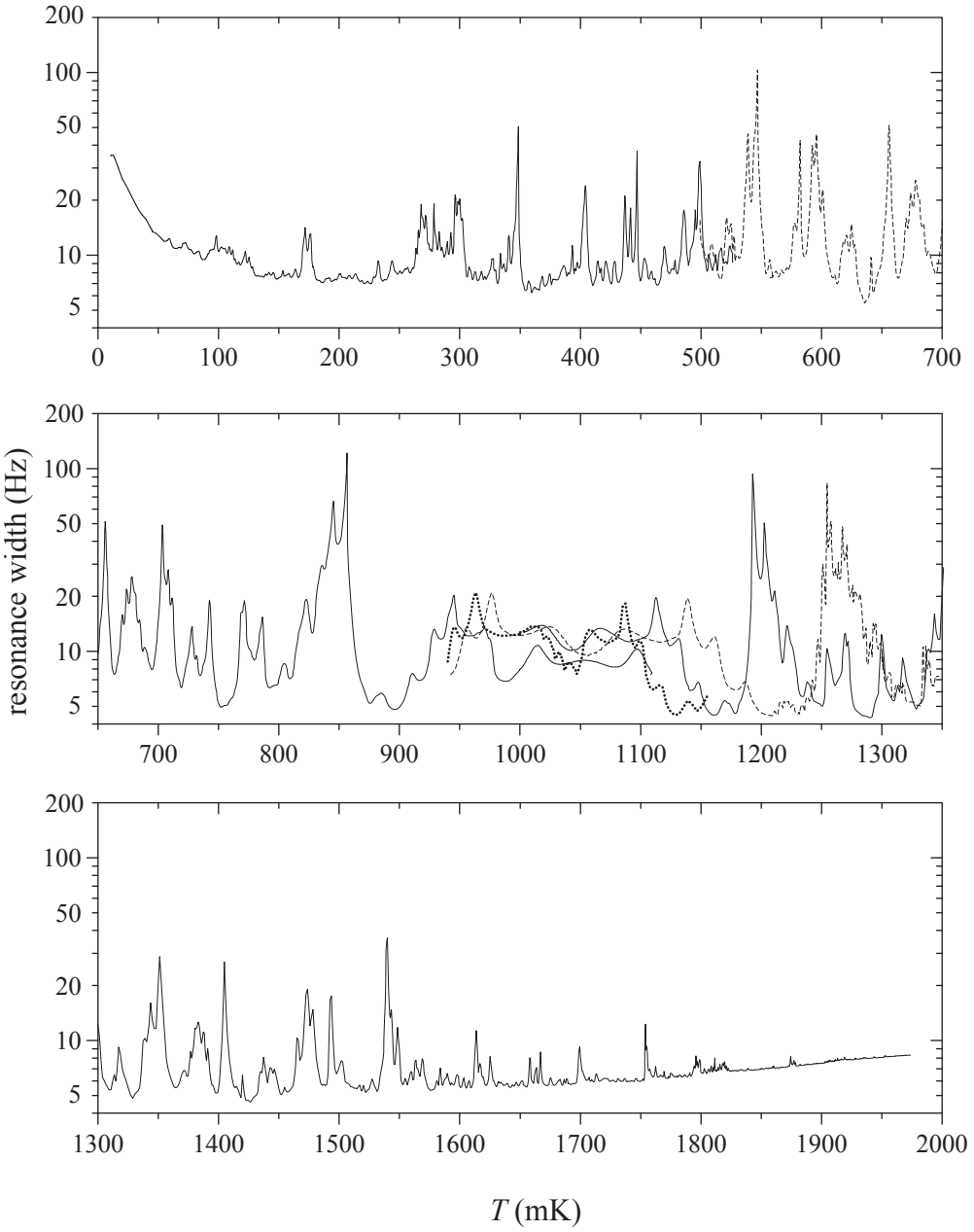

Fig. 2.9 Apparent resonance width of the tuning fork in helium mixture with about 8 % of ^{3}He. Concentration was varied slightly between measurements around 1 K, producing the differences in the data presented by different lines.

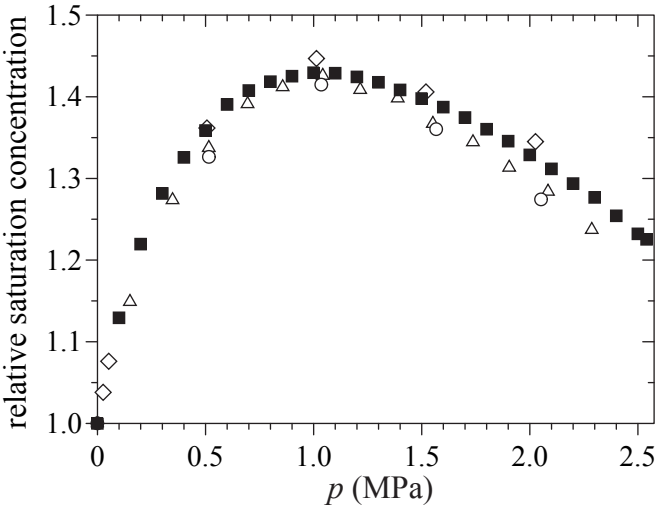

Fig. 2.10 Saturation concentration of ^{3}He in the dilute mixture, relative to the low-pressure value. Our results at 10 mK (■) and data by Watson *et al.* at 50 mK [34] (△), Landau *et al.* at zero-T limit [35] (◇), and Yorozu *et al.* at zero-T limit [36] (○).

mass density of the mixture, because the frequency and width change according to that ratio in response to small changes in temperature. Figure 2.10 shows the resulting low-temperature saturation concentration together with some earlier published data. Saturation concentrations have been plotted as relative to the zero-pressure value because of the low absolute accuracy of our measurement owing to the uncertainty in the volume of the mixture.

In addition to the pressure dependence of the saturation concentration in the zero-temperature limit, we also studied its temperature dependence. Up to some 100 mK, the temperature dependence is presumably quadratic and characterized by a pressure-dependent coefficient β according to

$$x_s(p,T) = x_s(p,0)\left(1+\beta(p)T^2\right). \tag{2.2}$$

Two kinds of tuning fork measurements were used to determine β at different pressures: temperature sweeps and pressure sweeps.

In a temperature sweep measurement, a sample with saturated mixture and a minute amount of pure ^{3}He was warmed up until completely mixed as a result of increased solubility, and then cooled down again. When cooling, the sample remained supersaturated across a certain range of temperatures before returning to the phase-separated state, which allowed determining the rate of change of the saturation concentration during warming by comparison to the constant supersaturation concentration.

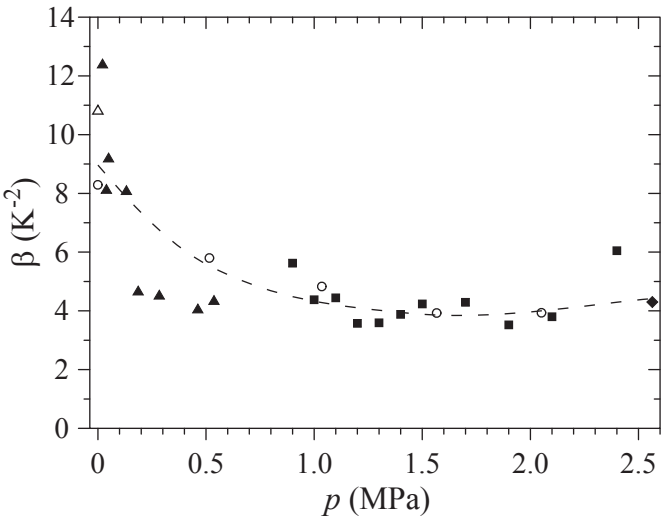

Fig. 2.11 Temperature coefficient β of the saturation concentration, determined by pressure sweeps (▲), temperature sweeps (■), and from the melting pressure (♦). Previous results by Yorozu *et al.* [36] (○) and Edwards *et al.* [37] (△).

In a pressure sweep measurement, a similar mixing-supersaturation-separation cycle of the sample was produced at constant temperature by first raising and then lowering pressure. The pressure of exact mixing was found as the pressure at which fork data for phase-separated and supersaturated mixtures intersected, and with this pressure measured at a few temperatures for a certain amount of ^{3}He, β could be calculated. The pressure sweep method was applicable for samples with a ^{3}He content such that the pressure of complete mixing was clearly below the pressure of maximum solubility.

Figure 2.11 shows the values of β obtained by temperature and pressure sweeps, a value at the melting pressure based on our analysis of the temperature dependence of the melting pressure of saturated mixture, and results of two previous authors [36, 37].

2.3 Melting pressure of ^{4}He in dilute helium mixture

Measurements of the melting pressure of dilute helium mixtures were conducted during both experiments discussed above, employing the same differential pres-

sure transducer. In the adiabatic melting experiment, measurements focussed on the use of the melting pressure for thermometry of the saturated mixture, in particular in the sub-millikelvin regime, whereas in the tuning fork experiment, several concentrations between zero and saturation were studied, mostly between 10 and 100 mK. The melting pressure of the saturated mixture is of special interest because, generally, an equilibrium system of one solid and two liquid phases of a binary mixture is univariant, *i.e.*, there is only one free thermodynamical variable that determines all others uniquely. In our case, this practically means that when temperature varies, the presence of the solid phase fixes pressure and the presence of the pure ^{3}He phase keeps the concentration of the mixture phase at saturation.

The melting pressure of a helium mixture, or the equilibrium pressure of its coexisting solid and liquid phases, is determined by the equality of the chemical potentials of the helium isotopes in different phases. Because at millikelvin temperatures, the solid phase can be assumed to consist purely of ^{4}He, and the entropy of ^{3}He in the liquid phase(s) is dominant and proportional to T, the melting pressure can be shown to have a constant derivative with respect to temperature squared, obeying

$$\frac{\mathrm{d}p_m}{\mathrm{d}(T^2)} = \frac{\pi^2 x R}{6(v_4^D - v_4^S)(1+\alpha x)T_F^D} \tag{2.3}$$

below saturation concentration, and

$$\frac{\mathrm{d}p_m}{\mathrm{d}\,(T^2)} = \frac{\pi^2 x R}{4v}\left(\frac{1}{T_F^D} - \frac{1}{T_F^R}\right), \tag{2.4}$$

derived in publication **II**, in the phase-separated mixture above the superfluid transition temperature T_c of ^{3}He. Temperatures below T_c will be discussed in the next section. In the equations above, R is the molar gas constant, T_F^D and T_F^R are the Fermi temperatures of ^{3}He in the dilute mixture and in the rich (essentially pure) liquid phase, α is the "^{3}He volume surplus" parameter introduced by Bardeen, Baym, and Pines [38], v_4^D and v_4^S are molar volumes of ^{4}He in the dilute mixture and in the solid, respectively, and v is defined

$$v = x(v_3^D - v_3^R) + (1-x)(v_4^D - v_4^S), \tag{2.5}$$

with v_3^D and v_3^R molar volumes of ^{3}He in the dilute mixture and rich phase, respectively. At the melting pressure, $\alpha \approx 0.165$ and $x \approx 0.082$. The linearity in T^2 was well realized in our experiments [19].

2.3.1 Effect of superfluidity of ^{3}He

As mentioned above, Eq. (2.4) for the melting pressure of a phase-separated mixture holds only above T_c, when the pure ^{3}He phase present is in the normal Fermi liquid state with entropy proportional to temperature. Below the superfluid transition, its entropy decreases more rapidly, approximately as $T^{2.67}$ according to specific heat data measured by Greywall [15]. This simple power-law approximation is appropriate between $T_c/2$ and T_c, and below that, while the entropy actually decreases exponentially, is adequate for this treatment as the entropy of the superfluid becomes negligibly small in comparison with that of the dilute mixture. With this correction below T_c taken into account, the melting pressure of the phase-separated mixture assumes a piecewise defined expression

$$p_m(T) = \begin{cases} p_0 + \frac{\pi^2 xR}{2v}\left(\frac{T^2}{2T_F^D} - \frac{T^{3.67}}{3.67 T_c^{1.67} T_F^R}\right), \; 0 < T \leq T_c \\ p_m(T_c) + \frac{\pi^2 xR}{4v}\left(\frac{1}{T_F^D} - \frac{1}{T_F^R}\right)(T^2 - T_c^2), \; T > T_c \end{cases}, \tag{2.6}$$

where $p_0 = 2.564$ MPa is the melting pressure at $T = 0$.

During the adiabatic melting experiment, measurements of the melting pressure of the saturated mixture below and around T_c were performed by first creating the solid at a temperature notably above T_c and blocking the superleak, then cooling the cell by nuclear demagnetization to below T_c, and finally letting it warm up slowly. Figure 2.12 presents the results of three such measurements, plotting the pressure, relative to the reference melting pressure of pure ^{4}He, as a function of the square of the temperature of the cell wall, measured by the Pt-NMR thermometer. For improved comparability, constant offsets have been applied to two of the data sets: $+5.7$ Pa to the data represented by circles and -7.2 Pa to the data represented by gray diamonds. Pressure differences of that order may arise from variation in the height of the solid, because the measured pressure is lower than the actual melting pressure by the hydrostatic pressure of the liquid between the membrane of the pressure transducer and the liquid–solid interface.

The apparent hysteresis in the plotted data, with pressures during cooling lying above those measured during warming, results from the temperature of helium lagging behind that of the thermometer due to the thermal boundary resistance at the cell wall. In the data represented by gray diamonds, the cusps during cooling occur when the demagnetization was interrupted to let the sample thermalize with the nuclear stage. Warming proceeded much slower than cooling so that the temperature lag is smaller in the lower branch of the data, decreasing with increasing temperature with estimated upper limits of 10% at 1 mK and 1% at

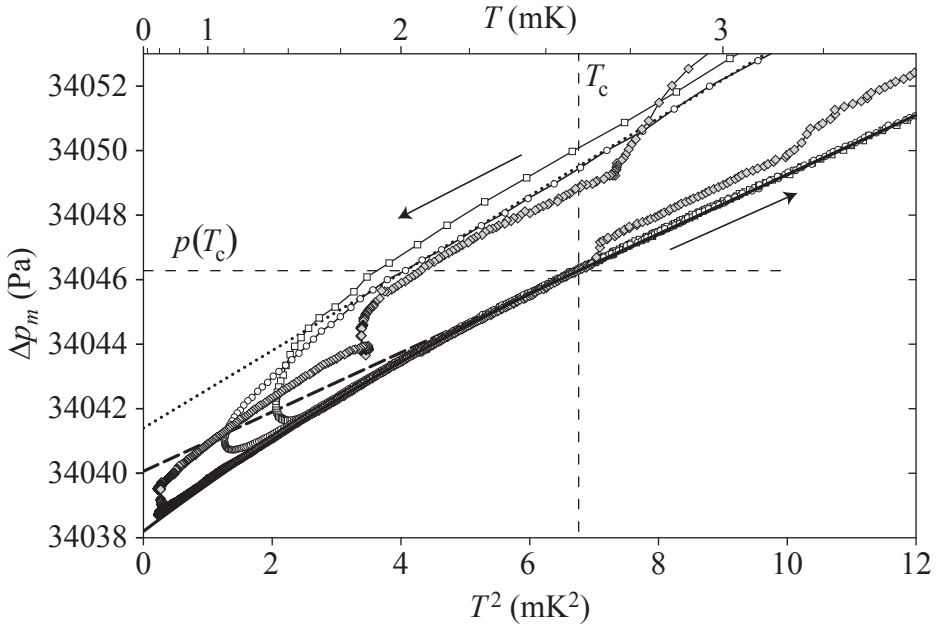

Fig. 2.12 Melting pressure measurements of three different crystals in phase-separated mixture across the superfluid transition of ^{3}He. Arrows indicate the direction of time.

2 mK. Because the warming data represent the actual temperature dependence of the melting pressure more accurately, the offsets have been chosen so that those parts fall on the same solid curve, calculated by Eq. (2.6) using the following parameter values: $T_F^R = 1.21$ K and $v = 2.05$ cm^3/mol, based on Refs. [23, 34, 39], and $p_0 = 34038.2$ Pa (here denoting difference to the melting pressure of pure ^{4}He), $T_F^D = 0.48$ K, $T_c = 2.6$ mK, and $x = 0.073$, determined by fitting. The downward deviation from the linear behavior above T_c (continued by the thick dashed line) is notable and corresponds to theory. The dotted line is to show that during cooling, the pressure data can also be seen to bend downwards from a linear dependence on T^2 after passing the pressure corresponding to T_c.

2.3.2 Osmotic pressure of helium mixture

The difference of the melting pressures of pure ^{4}He and dilute helium mixture is related to the osmotic pressure of ^{3}He in the mixture, a property measurable by other means at any pressure, and linking a macroscopic quantity to the microscopic description of the atomic interactions in the mixture through the chemical potential [**IV**]. The relation between the melting pressure difference Δp_m and

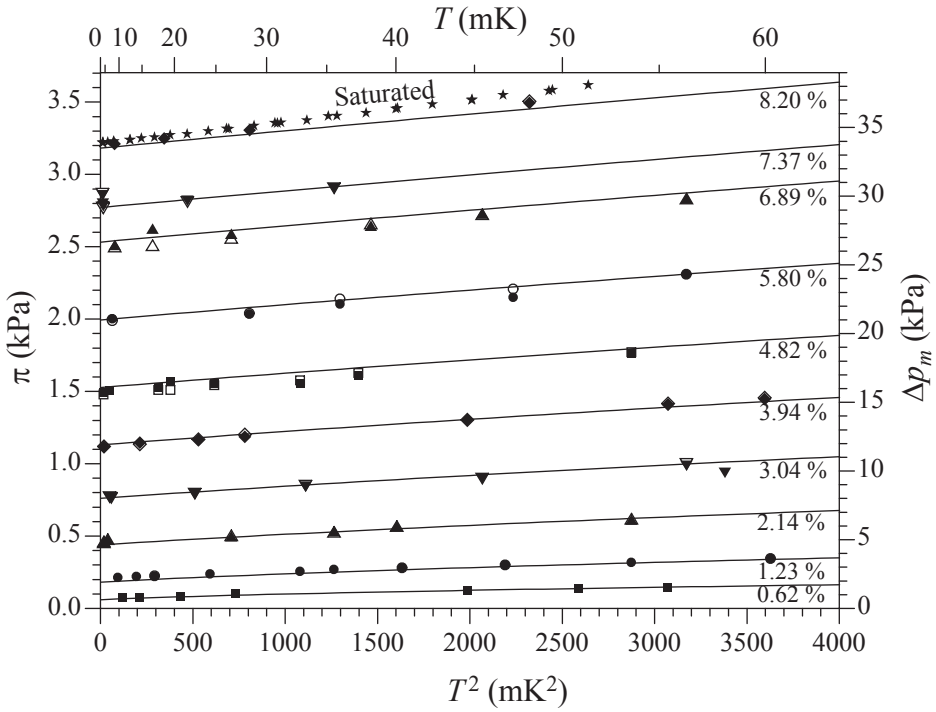

Fig. 2.13 Melting pressures (scale on the right) and derived osmotic pressures (scale on the left) of helium mixtures with indicated ^{3}He concentrations and of saturated mixture. Solid symbols refer to values based on the onset of solidification, and hollow ones to the disappearance of a melting solid.

osmotic pressure π is a simple proportionality by a ratio determined by molar volumes of liquid (v_4^L) and solid (v_4^S) ^{4}He:

$$\pi = \frac{v_4^L - v_4^S}{v_4^L} \Delta p_m \approx 0.09498 \Delta p_m. \tag{2.7}$$

Figure 2.13 shows the results of the melting pressure measurements in the test cell, with vertical scales for both the bare melting pressure, on the right, and the osmotic pressure, on the left. The mixture samples, with concentrations at the melting pressure shown in the plot, were the same that were used to study the response of the tuning fork and ^{3}He solubility in mixtures. The figure also presents theoretical curves for each concentration, calculated by Rysti using a model potential for the effective interaction of ^{3}He quasiparticles in the mixture [40, 41].

Chapter 3

Conclusions

Cooling dilute mixture of ^{3}He in ^{4}He by adiabatic melting of ^{4}He has been studied for the first time in the sub-millikelvin regime, where the method can, in principle, reach mixture temperatures significantly lower than attainable by the conventional approach with an external or immersed nuclear coolant. In the experiment, cooling was detected, using a vibrating wire resonator in the superfluid ^{3}He phase as a thermometer, at temperatures down to about 0.3 mK. Even though the decrease of temperature caused by the adiabatic melting process remained at a modest level, the results can be considered promising at this stage of the development of the method, as the reasons for the limited performance were, evidently, technical rather than fundamental. A simulation of one of the cooling attempts indicates that when all known shortcomings are taken into account, the observed behavior agrees with theory. Therefore, cooling results can be expected to improve notably in future experiments if the two main technical difficulties, related to the superleak line and to thermal coupling, are overcome.

The superleak line for transfer of ^{4}He into and out of the cell did not allow as high flow rates as intended without dissipation, and even for smooth flow at low rates, special flushing of the line was necessary. This is likely to result from a defective structure of the superleak line, such as hollows in which solidification of ^{4}He is possible. The most probable location of such defects were joints at a couple of thermalization posts along the superleak. New superleaks of improved continuous design have been constructed and tested for use in a planned continuation of the experiment. In addition to increasing the maximum outward ^{4}He flow rate, the new design should also enable more complete solidification of ^{4}He in the cell, as any remaining liquid mixture constitutes a parasitic heat capacity.

The thermal boundary resistance between the cell body and the helium sample proved lower than desired, especially given the limited rate of melting ^{4}He. It

was intended that the boundary resistance, rapidly increasing with falling temperature, would effectively decouple the sample from the body so that the cooling power produced by the adiabatic melting would only be used to cool down the sample itself, not the surrounding structures. To ensure better thermal decoupling in the next setup, an arrangement is under construction in which the sample is divided into two compartments, one with the sintered metal heat exchanger and the other for the process of adiabatic melting, and conduction of heat through a channel connecting these compartments will be adjustable by a valve or at least optimized to provide a sufficient precooling capability without compromising performance in the final stage of the cooling.

Direct thermometry of the helium sample by its melting pressure and by mechanical oscillators was also studied, both as a part of the adiabatic melting experiment and in a later test setup. Melting pressure was measured capacitively by a differential pressure transducer with the melting pressure of ^{4}He as a reference, reaching a superb resolution enabling melting pressure thermometry down to some 0.1 mK. The effect of the superfluidity of ^{3}He on the melting pressure of the saturated mixture was observed and successfully described in simple thermodynamical terms. Combining the understanding of the temperature dependence of the melting pressure with the ability to measure the pressure accurately with aim at practical thermometry requires awareness of the fact that in the sub-millikelvin regime, contribution from hydrostatic pressure, dependent on the amount of solid in the cell, surpasses the temperature dependence of the melting pressure.

In the adiabatic melting experiment, the established vibrating wire technique was applied, whereas in the test cell, a commercial quartz tuning fork served as an oscillating probe of the helium sample. The sensitivity of the fork to the mass density and viscosity of the surrounding fluid was studied and exploited to measure, for example, the pressure and temperature dependence of the saturation concentration of ^{3}He in ^{4}He, for the first time up to the melting pressure of the mixture. In addition to the monotonous temperature dependence of viscous damping, similar to what is experienced by vibrating wires, fork measurements in helium mixtures revealed that the oscillator is strongly influenced by second sound, or concentration waves, in the mixture. This appears as a spectrum of peaks in the damping of the fork, each peak corresponding to a resonant mode of second sound. This is a disturbing irregularity with respect to measurement of density, or to viscosity-based thermometry, but, on the other hand, offers an interesting prospect of using the sharp peaks occurring at certain values of temperature as reference points.

References

[1] G.-H. Oh, Y. Ishimoto, T. Kawae, M. Nakagawa, O. Ishikawa, T. Hata, and T. Kodama, J. Low Temp. Phys. **95**, 525 (1994).

[2] E. Pentti, Master's thesis, Helsinki University of Technology (2003).

[3] W. Yao, T. A. Knuuttila, K. K. Nummila, J. E. Martikainen, A. S. Oja, and O. V. Lounasmaa, J. Low Temp. Phys. **120**, 121 (2000).

[4] T. Knuuttila, Ph.D. thesis, Helsinki University of Technology (2000).

[5] J. Tuoriniemi, K. Juntunen-Nurmilaukas, J. Uusvuori, E. Pentti, A. Salmela, and A. Sebedash, Nature **447**, 187 (2007).

[6] D. I. Bradley, S. N. Fisher, A. M. Guénault, R. P. Haley, and G. R. Pickett, J. Low Temp. Phys. **135**, 385 (2004).

[7] B. Castaing, A. S. Greenberg, and M. Papoular, J. Low Temp. Phys. **47**, 191 (1982).

[8] R. L. Rusby, M. Durieux, A. L. Reesink, R. P. Hudson, G. Schuster, M. Kühne, W. E. Fogle, R. J. Soulen, and E. D. Adams, J. Low Temp. Phys. **126**, 633 (2002).

[9] J. Martikainen and J. T. Tuoriniemi, J. Low Temp. Phys. **124**, 367 (2001).

[10] J. Martikainen, J. Tuoriniemi, T. Knuuttila, and G. Pickett, J. Low Temp. Phys. **126**, 139 (2002).

[11] J. Martikainen, J. Tuoriniemi, E. Pentti, and G. Pickett, in *Proceedings of the 23rd International Conference on Low Temperature Physics* (Elsevier, Amsterdam, 2003), vol. 329-333 of *Physica B*, pp. 178–179.

[12] R. Blaauwgeers, M. Blazkova, M. Človečko, V. B. Eltsov, R. de Graaf, J. Hosio, M. Krusius, D. Schmoranzer, W. Schoepe, L. Skrbek, et al., J. Low Temp. Phys. **146**, 537 (2007).

[13] D. O. Clubb, O. V. L. Buu, R. M. Bowley, R. Nyman, and J. R. Owers-Bradley, J. Low Temp. Phys. **136**, 1 (2004).

[14] D. O. Edwards and S. Balibar, Phys. Rev. B **39**, 4083 (1989).

[15] D. S. Greywall, Phys. Rev. B **33**, 7520 (1986).

[16] A. P. Sebedash, JETP Lett. **65**, 276 (1997).

[17] V. N. Lopatik, Sov. Phys. JETP **59**, 284 (1984).

[18] A. Salmela, Master's thesis, Helsinki University of Technology (2006).

[19] A. Sebedash, J. T. Tuoriniemi, S. Boldarev, E. M. Pentti, and A. J. Salmela, in *Low Temperature Physics: 24th International Conference on Low Temperature Physics – LT24* (AIP, New York, 2006), vol. 850 of *AIP Conf. Proc.*, p. 1591.

[20] Fox Electronics, Fort Myers, Florida, USA, URL `http://www.foxonline.com`.

[21] J. N. Newman, *Marine hydrodynamics* (MIT Press, Cambridge, Massachusetts, USA, 1977).

[22] E. Tanaka, K. Hatakeyama, S. Noma, and T. Satoh, Cryogenics **40**, 365 (2000).

[23] M. Kollar and D. Vollhardt, Phys. Rev. B **61**, 15347 (2000).

[24] R. D. McCarty, Technical Note 631, National Bureau of Standards, Gaithesburg, Maryland, USA (1972).

[25] R. J. Donnelly and C. F. Barenghi, J. Phys. Chem. Ref. Data **27**, 1217 (1998).

[26] H. Højgaard Jensen, H. Smith, P. Wölfle, K. Nagai, and T. Maack Bisgaard, J. Low Temp. Phys. **41**, 473 (1980).

[27] D. C. Carless, H. E. Hall, and J. R. Hook, J. Low Temp. Phys. **50**, 583 (1983).

[28] A. M. Guénault, V. Keith, C. J. Kennedy, and G. R. Pickett, Phys. Rev. Lett. **50**, 522 (1983).

[29] C. T. Lane, H. A. Fairbank, and W. M. Fairbank, Phys. Rev. **71**, 600 (1947).

[30] R. D. Maurer and M. A. Herlin, Phys. Rev. **76**, 948 (1949).

[31] D. de Klerk, R. P. Hudson, and J. R. Pellam, Phys. Rev. **93**, 28 (1954).

[32] J. C. King and H. A. Fairbank, Phys. Rev. **93**, 21 (1954).

[33] N. R. Brubaker, D. O. Edwards, R. E. Sarwinski, P. Seligmann, and R. A. Sherlock, J. Low Temp. Phys. **3**, 619 (1970).

[34] G. E. Watson, J. D. Reppy, and R. C. Richardson, Phys. Rev. **188**, 384 (1969).

[35] J. Landau, J. T. Tough, N. R. Brubaker, and D. O. Edwards, Phys. Rev. A **2**, 2472 (1970).

[36] S. Yorozu, M. Hiroi, H. Fukuyama, H. Akimoto, H. Ishimoto, and S. Ogawa, Phys. Rev. B **45**, 12942 (1992).

[37] D. O. Edwards, E. M. Ifft, and R. E. Sarwinski, Phys. Rev. **177**, 380 (1969).

[38] J. Bardeen, G. Baym, and D. Pines, Phys. Rev. **156**, 207 (1967).

[39] A. Driessen, E. van der Poll, and I. F. Silvera, Phys. Rev. B **33**, 3269 (1986).

[40] J. Rysti, Master's thesis, Helsinki University of Technology (2008).

[41] Anssi Salmela, Alexander Sebedash, Elias Pentti, Juho Rysti, and Juha Tuoriniemi, to be published.

Abstracts of publications

I **Towards Superfluidity of ^{3}He Diluted by ^{4}He**

Search for the superfluid state of dilute ^{3}He dissolved to ^{4}He is one of the major remaining problems of low temperature physics. We describe our two experiments designed to pursue the lowest achieved temperature in such mixtures essentially below the values reported before.

II **Melting Pressure Thermometry of the Saturated Helium Mixture at Millikelvin Temperatures**

The melting pressure of a ^{3}He-^{4}He mixture has a very simple quadratic temperature dependence below some tens of mK, determined by the entropy of the ^{3}He component in the liquid mixture. For undersaturated mixtures, the melting pressure also depends on the ^{3}He concentration x, which may vary in the course of the experiment as ^{4}He transfers between the liquid and the solid phases. On the other hand, if the mixture is saturated, the system is in a univariant state with a melting pressure that depends uniquely on temperature and, thus, offers a thermometric standard. However, the univariant state includes a pure liquid ^{3}He phase, which complicates the temperature dependence around its superfluid transition temperature T_c. In this paper, we analyze the melting pressure of the saturated mixture in simple terms and find an expression that is in good agreement with our experimental data, and is applicable across T_c down to very low temperatures. The obtained derivatives of the melting pressure with respect to the square of temperature are 0.92 Pa·mK^{-2} above T_c and 1.52 Pa·mK^{-2} in the zero-temperature limit.

III **Adiabatic Melting of ^{4}He Crystal in Superfluid ^{3}He at Sub-millikelvin Temperatures**

Adiabatic melting of ^{4}He crystal to phase separated ^{3}He-^{4}He solution (at $T <$ 2 mK) is probably the most promising method to cool the dilute phase down to temperatures substantially below 0.1 mK. When started well below the superfluid transition temperature T_c of pure ^{3}He, this process allows, in principle, to get the final temperature (T_f) several orders of magnitude less than the initial one (T_i). This work is the first practical implementation of the method below the T_c of ^{3}He. The observed cooling factor was $T_i/T_f = 1.4$ at 0.9 mK, being mainly limited by the bad performance of the superleak filling line, by incomplete solidification of ^{4}He in the cell, and by the improper thermal contact between the cell wall and the liquid.

IV **Osmotic Pressure of ^{3}He–^{4}He Solutions at 25.3 Bar and Low Temperatures**

The osmotic pressures of dilute ^{3}He-^{4}He solutions were determined at 25.3 bar from measurements of crystallization curves at temperatures from 5 mK to 60 mK, when the ^{3}He component of the solution obeying the Fermi-Dirac statistics

was deep in the degenerate state. We determine the shift of the crystallization pressure of the solution of interest relative to pure ^{4}He when both these substances are present in the cell in two separate volumes at the same temperature. We used our novel ultra-sensitive capacitive gauge for measurements of small pressure differences between the two substances. We used a quartz resonator for determination of solution's concentration in situ. The difference between the crystallization pressure of the saturated solution and pure ^{4}He, both extrapolated to zero temperature, is (339$\pm$2) mbar.

V Quartz Tuning Fork in Helium

Use of a quartz tuning fork for precise measurements of density has been studied in normal ^{3}He liquid and in ^{4}He liquid and vapor, spanning a reasonably wide range of fluid densities. It is evident that the compressibility of the fluid must be accounted for in order to properly interpret the resonator response.

VI Solubility of ^{3}He in ^{4}He at millikelvin temperatures up to the melting pressure measured by a quartz tuning fork

We have studied dilute liquid mixtures of ^{3}He in ^{4}He at millikelvin temperatures to find the maximum solubility in the zero-temperature limit, covering for the first time the whole pressure range of the liquid phase. Injecting pure ^{4}He into the sample cell through a superleak made it possible to pressurize the mixture up to the melting curve at low temperatures, unattainable through ordinary capillaries due to the minimum of the melting pressure which would block any customary filling lines at around 1 K. The possibility to selectively drain ^{4}He out of the cell through the superleak enabled us to reversibly cover the full span of pressures with a given amount of ^{3}He in the system and to add ^{3}He into the sample volume through an ordinary filling line without the necessity to warm up in between, thus probing the concentration range in small steps in one continuous run in an unprecedented way. Here we report the results on the pressure and temperature dependence of the saturation concentration of the mixture, based on the response of an oscillating quartz tuning fork immersed in the helium mixture. Our data generally agree with earlier results, but suggest that above the solubility maximum around 10 bar the decrease in the saturation concentration as a function of pressure is not as steep as observed in earlier capacitive concentration measurements.

VII Studies on helium liquids by vibrating wires and quartz tuning forks

We present results of low-temperature experiments on dilute mixtures of ^{3}He in ^{4}He and on pure ^{3}He, obtained by means of two kinds of mechanical oscillators immersed in the liquid sample: vibrating wires and quartz tuning forks. The measured effect of the surrounding fluid on the mechanical resonance of the oscillators is compared with existing theories. We also discuss resonances of second sound and the state of supersaturation, both observed by a tuning fork in helium mixtures.

ISBN 978-952-248-020-0
ISBN 978-952-248-021-7 (PDF)
ISSN 1795-2239
ISSN 1795-4584 (PDF)